atmosphere

MDPI

Article

Land-Use Regression Analysis of Summer Tropospheric Ozone Concentrations in Ireland

Keelan McHugh [1,*], Thomas Cummins [1] and Julian Aherne [2]

[1] UCD School of Agriculture and Food Science, University College Dublin, D04 N2E5 Dublin, Ireland; thomas.cummins@ucd.ie
[2] School of Environment, Trent University, Peterborough, ON K9L 0G2, Canada
* Correspondence: keelan.mc-hugh@ucdconnect.ie

Abstract: Tropospheric ozone is a powerful oxidant that can damage living organisms; it is widely monitored, as air concentrations have more than doubled since the Industrial Revolution. However, in general air quality monitoring stations are limited spatially to large urban centres; accordingly, accurate prediction of concentrations outside of cities is important for protecting human and plant health. Land-use regression has been successfully used for modelling air pollutant concentrations by establishing a relationship between observed concentrations and landscape features representing sources and sinks. In this study, we developed a land-use regression model that explained 68% of the variance of summer average ozone concentrations in the Republic of Ireland. Ozone was measured at 14 active and 20 passive monitoring sites; air concentrations varied spatially, with the highest ozone measured in rural upland (64.5 μg/m^3) and Atlantic coastal (50.2–60.5 μg/m^3) sites and the lowest generally in urban centres (38.9–45.7 μg/m^3). A total of 74 land-use predictor variables were tested, and their inclusion in the model was based on their impact on the coefficient of determination (R^2). The final model included variables linked primarily to deposition processes and included "forest woodland and scrub area" and "distance to coast". The meteorological variable "rain" and an indicator for NO_x emissions "distance to EPA Integrated Pollution Control facilities" were also included in the final model. Our results demonstrate the potential effectiveness of land-use regression modelling in predicting ozone concentrations, at a scale relevant for ecosystem protection.

Keywords: passive samplers; R^2; intercept; modelled ozone; deposition

Citation: McHugh, K.; Cummins, T.; Aherne, J. Land-Use Regression Analysis of Summer Tropospheric Ozone Concentrations in Ireland. *Atmosphere* **2023**, *14*, 1711. https://doi.org/10.3390/atmos14121711

Academic Editor: Nima Afshar-Mohajer

Received: 3 October 2023
Revised: 8 November 2023
Accepted: 17 November 2023
Published: 21 November 2023

1. Introduction

Tropospheric or 'ground-level' O_3 is a powerful oxidant that is harmful to human [1,2] and plant [3] health. In vegetation, O_3 enters through the leaf stomata, initiating a plant-derived oxidative burst leading to damage, which reduces photosynthesis and negatively impacts plant growth and ecosystem health [4–6]. Further, O_3 is an important greenhouse gas [7] due to its properties as a radiative forcer. Ground-level O_3 is a secondary pollutant as it is not emitted directly but formed in the atmosphere from the reaction of precursor compounds, including nitrogen oxides (NO_x) and volatile organic compounds (VOCs), in the presence of sunlight. As such, O_3 concentrations are highly variable over space and time due to the complex nonlinear processes of chemical creation from precursors, destruction through titration, and removal by deposition. Nitrogen oxides in the form of either nitric oxide (NO) or nitrogen dioxide (NO_2) are mainly produced by the combustion of fossil fuels, with power generation and motor vehicle emissions being the dominant sources [8], much larger than formation by lightning [9]. In addition to biogenic emissions, anthropogenic sources of VOCs include emissions from the incomplete combustion of fossil fuels and from agricultural organic and inorganic fertilisers, solvents, and adhesives [8]. It is well established that O_3 production increases with increasing concentrations of NO_x and VOCs, where the emissions of both precursors are not limited, and increases less as the regime

becomes NO_x- or VOC-limited [10–12]. Ground-level O_3 tends to be lower in urban areas due to removal by fresh traffic emissions of NO, leading to a downward flux gradient and a VOC-limited regime, meaning less formation of O_3 [13,14]. In these regimes, a reduction in the emissions of NO_x can lead to a transitional regime with increases in O_3 formation [15]. This process was evident during COVID-19 restrictions when NO_x emissions from traffic were reduced, resulting in increased O_3 concentrations in European cities [16]. Further, O_3 can be removed through dry deposition to surfaces, and the rate of O_3 removal by deposition decreases with temperature [17] and increases with surface roughness, e.g., forests have higher rates of O_3 removal than open water [18–20]. This deposition takes place in the form of uptake in plant stomata and non-stomatal destruction through surface contact and chemical destruction [17], with non-stomatal deposition dominating during drought conditions [21].

One of the challenges of estimating regional O_3 concentrations is its variability, often varying with altitude, geographic location, season, temperature, humidity, and atmospheric composition [22]. The global average photochemical lifetime of tropospheric O_3 is 20 to 25 days [23] but generally less than 5 days in the summertime surface boundary layer, with considerable spatial variation. In contrast, the lifetime of O_3 is long enough in the free troposphere to allow for long-range transport [24], with high emissions in one area influencing concentrations far from the source.

In Europe, the highest concentrations are observed along the Mediterranean [25], and the lowest concentrations in cities [16]. Similarly, on the Atlantic edge of Europe, in the Republic of Ireland, the highest concentrations are experienced at stations along the west coast, and the lowest in the cities [26]. In Ireland, O_3 levels increased during the 1990s until the year 2000, and thereafter levelled off up to the year 2008 [27,28]. However, this plateau was short-lived, as almost half of the stations measuring ozone had significant increases during the 15-year period 2005–2019 [26]. Increases were most frequent in winter with significant increases at seven stations, while three stations in rural and coastal locations had significant increases during the spring period, when peak values occurred.

Given the negative impacts of exposure to high levels of O_3, it is important to effectively predict O_3 exposure especially where monitoring data are not available. There are currently 24 stations measuring O_3 in the Republic of Ireland (area: 70,273 km^2). This spatial paucity of O_3 monitoring makes the accurate prediction of concentrations at fine spatial scales difficult, due to the wide range of local influences that determine concentrations at a given location. Land-use regression (LUR) modelling has been widely used [29–34] to understand the relationship between air pollutant concentrations (response variable) and land-use characteristics (explanatory variables). Land-use regression is a prediction method that aims to maximise the explained variance (R^2) and has been successfully applied for NO_2, PM_{10}, and $PM_{2.5}$ [31], and for O_3 [35]. In Ireland, there is a growing need for a better understanding of the drivers of local-scale O_3 variations, and fine-scale concentration maps for the growing season to determine where exposure limits may be exceeded, especially given recent increasing O_3 trends.

The objectives of this study were to identify the covariates of summer O_3 concentrations in Ireland, and to develop a fine spatial-scale O_3 concentration map using LUR modelling. Firstly, O_3 passive samplers were deployed across Ireland during June–September 2022 in locations not represented by active monitoring stations. Secondly, each sample location (n = 34, including both active and passive) was characterised based on a wide, exploratory set of O_3-relevant predictor or explanatory variables such as land-use, traffic, and elevation. Thirdly, a regression model was created using measured O_3 data, and determinants were assessed based on maximizing the explained variance. The resulting model was used to map local O_3 levels across the country at a spatial scale needed for ecosystem protection (1 km × 1 km). In general, the sampling and modelling protocols used in this study followed those from the ESCAPE (European Study of Cohorts for Air Pollution Effects) project [29,31].

2. Materials and Methods

2.1. Sample Site Selection

In total, 34 sites across the Republic of Ireland were used in this study (see Figure 1). These included 14 active O_3 monitoring stations under the national monitoring network and 20 passive sampling locations, which were established to improve the spatial coverage of O_3 during summer (May–September) 2022. To maximise spatial coverage between the 14 long-term active monitoring sites, 16 short-term passive sampler locations were chosen from the centre of spatially balanced strata that were mapped using k-means clustering in R (see Figure S1; SPCOSA package; [36]). The passive sampling sites were supplemented with four additional sampling sites that were part of an ongoing O_3 vegetation experiment. The selected passive sampler locations were inspected for access and to select nearby power transmission poles that were free from airflow obstruction on all sides for sampler deployment. In locations near major roads, the nearest minor road was selected, to allow for safe access and to lessen the impact from local NO traffic emissions. All study sites were classified as urban, suburban, rural, or coastal.

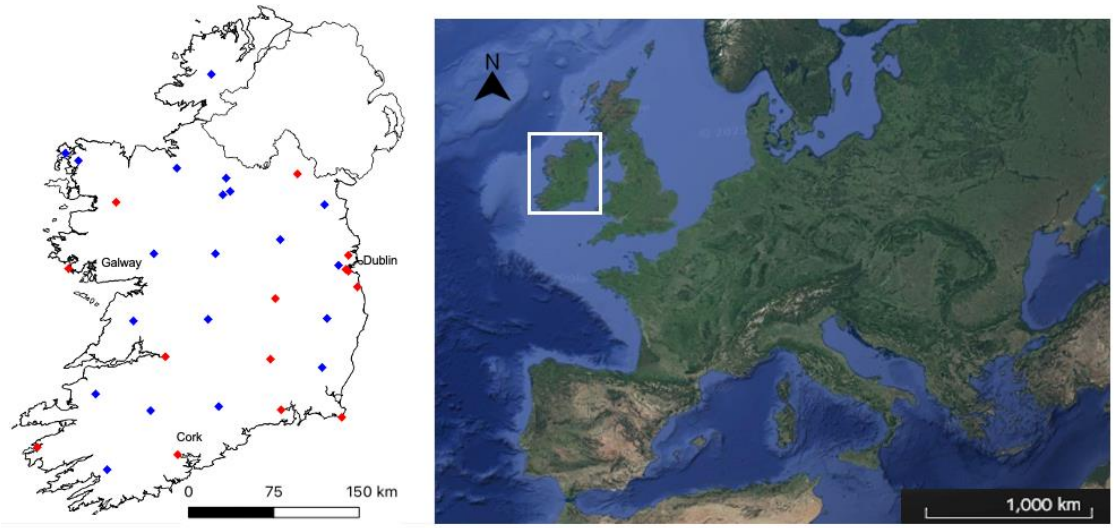

Figure 1. Location of Ireland within Europe with inset showing ozone monitoring sites in the Republic of Ireland used in the study (n = 34); red-filled diamonds indicate active monitoring stations (n = 14), and blue-filled diamonds indicate passive sampling sites (n = 20) established during summer 2022 to ensure national-scale coverage of ozone data.

2.2. Measurement of Ozone

Continuous tropospheric O_3 was measured using UV photometric analysers (Thermo 49i and API models (Thermo Fisher Scientific, Waltham, MA, USA)) and archived online under the national air quality monitoring network. Hourly O_3 concentrations were downloaded from the EPA SAFER database (https://eparesearch.epa.ie/safer/iso19115/display?isoID=66, accessed on 15 November 2023). To ensure that mean values were representative during the sampling period, the data were assessed for missing values and sites were included in the study if they met a data completeness threshold of 75%, as set out by the Tropospheric Ozone Assessment Report [37].

The average monthly tropospheric O_3 was also passively measured using "Palmes-type" diffusion tubes [38], where the reaction of O_3 with a nitrate-coated absorbent membrane in the passive sampler was quantified using ion chromatography. Tubes were made from fluorinated ethylene polymer and were fitted with two caps—one containing the absorbent and one containing a one-micron porosity filter to avoid airborne particulate nitrate from entering. The O_3 diffusion tubes used in this study were obtained from Gradko International (Winchester, UK), a UKAS (United Kingdom Accreditation Service) accredited laboratory. The diffusion tubes were exposed for four weeks, under three consecutive

deployments during June–September 2022 (referred to as the "summer period" in this study). Sampling sites covered a distance of more than 2000 km; therefore, deployment and sample changeover took four days. The first exposure began on the week of 13–19 June, with changeovers on 11–14 July and 8–11 August, and final collection on 5–8 September. At each site, one O_3 tube was attached vertically to a transmission pole at a height of 3 m to avoid interference and secured to the pole using a 20 cm spacer to allow free airflow around the diffusion tube. Deployment blanks were travelled during each exposure period, while laboratory blanks were not travelled. Measured passive concentrations may be elevated when tubes are exposed to intense direct sunlight due to the breakdown of NO and NO_2; as such, the tubes were also co-located at two active monitoring stations to facilitate calibration of passive sampling data. The passive data were separately calibrated for each exposure by reducing each value proportionally by the average percent difference between the co-located active and passive samplers (see Table S1). For each exposure, triplicate samplers were deployed at three different locations to assess variation among the tubes. Following the sampler collection, the diffusion tubes were returned to Gradko for analysis. Variation between sites and triplicate samples was assessed using percent coefficient of variation—calculated by dividing the standard deviation by the mean and multiplying by 100. The significance of the difference between the sampling periods was assessed using a Kruskal–Wallis test. The calibrated passive sampler concentrations during each period along with averaged data from the active monitoring stations was assessed for spatial and temporal variation.

2.3. Characterising Locations by Landscape Features

For each study location (n = 34), contributions of candidate determinants (predictor variables) to model R^2 were quantified. The predictor variables represent potential sources and sinks of O_3 concentrations such as land-cover, road type, altitude, and distance from the coast. In total, 74 predictor variables were used to build the LUR model. These predictor variables were selected based on their suspected relationship with O_3. Determinants were further divided based on different buffer sizes, where circles with radii ranging between 100 m and 5000 m were placed around the sample points and the determinant value was extracted within each buffer size (see Table 1 for variables and buffer sizes used). The buffers aimed to capture the spatial scale of impact from predictor variables and the dispersion patterns associated with O_3. The coordinates of each sample point were taken from Google Earth. The land cover data were extracted from the national land cover map for Ireland (https://www.tailte.ie/surveying/products/professional-mapping/national-land-cover-map/, accessed on 15 November 2023). A Geographical Information System was used to generate determinants such as distance from the coast and major roads for each study site. Emissions of CO, NH_3, nonmethane VOCs, NO_x, PM_{10}, $PM_{2.5}$, and CH_4 on a 1 × 1 km spatial scale for Ireland were obtained from the MapEire project ([39]; projects.au.dk/mapeire/spatial-results/, accessed on 15 November 2023; emissions based on 2017 data).

Table 1. List of predictor variables used for modelling ozone, with units and buffer sizes. Temperature, Rain, and Sun based on a 30-year mean.

Predictor Variable	Unit	Buffer Radius (m)
Easting	m	
Northing	m	
Elevation	m	
Maximum temperature	°C	
Minimum temperature	°C	
Mean temperature	°C	

Table 1. *Cont.*

Predictor Variable	Unit	Buffer Radius (m)
Rain	mm/year	
Sun	hour/year	
Distance to coast	m	
Distance to major road	m	
Distance to IPC facility	m	
Distance to EPA Licenced facility	m	
Distance to waste facility	m	
CO	tonne/year	
NH3	tonne/year	
NMVOC	tonne/year	
NO_x	tonne/year	
PM_{10}	tonne/year	
$PM_{2.5}$	tonne/year	
CH_4	tonne/year	
Population	person	100, 200, 300, 500, 1000, 5000
Buildings area	m^2	100, 200, 300, 500, 1000, 3000
Forest, woodland and scrub area	m^2	100, 200, 300, 500, 1000, 3000
Grass, marsh, swamp area	m^2	100, 200, 300, 500, 1000, 3000
Waterbodies area	m^2	100, 200, 300, 500, 1000, 3000
Total road length	m	100, 200, 300, 500, 1000, 5000
Secondary road length	m	100, 200, 300, 500, 1000, 5000
Service road length	m	100, 200, 300, 500, 1000, 5000
Tertiary road length	m	100, 200, 300, 500, 1000, 5000

2.4. Data Analysis and Model Building

The measured O_3 data and selected determinants were tested for normality using the Shapiro–Wilks test, and all determinants were log-transformed. As some determinants had zero values, a value of one was added to all the variables before transformation. While more than 80% of the determinant variables remained nonnormal after transformation (including four used in the final model), normality was nonetheless improved, and the response variable was normally distributed. Secondly, all the determinants were tested for correlation using the Pearson correlation to avoid multicollinearity in the model, and were considered colinear if the correlation coefficient was greater than 0.65. Finally, using a stepwise forward and backward procedure for model development, the determinants were evaluated with the aim to maximise the explained variance (R^2) for the measured summer O_3 concentration (using Kyplot, version 2.0; [40]). The determinants were separated and grouped into five uncorrelated groups, and one per group was sequentially introduced, with their impact on the R^2 value ultimately determining their inclusion in the final model. The process was repeated until all the variables were tested, and the adjusted R^2 value was maximised. To assess the individual impact of the final model determinants on the predicted concentrations, the values were normalised by dividing by their mean, allowing comparison of their regression coefficients. The top five regression models with the highest adjusted R^2 values were retained, and the final model was chosen based on the highest adjusted R^2 value. The final model was tested using a cross validation method [41], where 90% of the sites were selected at random and the model was developed using these sites and the selected determinants, with the remaining 10% of sites being used to validate the model. This process was repeated until all sites had been used for model testing.

3. Results and Discussion

3.1. Distributions of Measured Concentrations

Ozone concentrations varied spatially, with the highest concentrations measured in rural and Atlantic coastal sites and the lowest concentrations measured at urban sites. Active and passive mean concentrations ranged between 38.8 and 64.5 $\mu g/m^3$ (see Table 2). The mean value for all the station concentrations was 50.7 $\mu g/m^3$, with a standard deviation

of 5.96 μg/m^3 and coefficient of variation of 17%, indicating a low level of variability between stations. Across the three exposures, the highest concentrations were measured during the third exposure (see Figure 2), and the first exposure was significantly different (lower concentration) to the second (p-Value = 0.01) and third (p-Value < 0.001). Laboratory and deployment blanks had a mean O_3 value < 1 μg/m^3; as such, observations were not blank-corrected. Passive O_3 concentrations at co-located sites were on average 21–29% higher each month than the active concentrations during the same period (see Table S1). Triplicate samples taken from four sample locations had low variability, with a mean coefficient of variation of 6%. Sampler recovery was 96% during the study, as one site (Wexford) had samples removed during the third exposure.

Table 2. Site details of passive and active sites used in the study with mean measured ozone concentration (μg/m^3) during summer (May–September) 2022.

Site	Latitude	Longitude	Elevation	Sampling Method	Site Classification	Measured O_3
			m			μg/m^3
Athlone	53.458388	−7.9797343	34	Passive	Rural	46.6
Ballinamore	54.046680	−7.8395779	89	Passive	Rural	47.4
Belmullet	54.220789	−9.9907000	5	Passive	Atlantic	60.5
Belmullet east	54.168465	−9.8176626	24	Passive	Rural	58.1
Bray	53.187458	−6.1227087	47	Active	Sub-urban	48.7
Carnsore point	52.177439	−6.3677987	5	Active	Rural	53.2
Castlebar	53.850875	−9.3001777	40	Active	Sub-urban	46.1
Clare	52.930413	−9.0481050	24	Passive	Rural	46.8
Clonskeagh	53.311796	−6.2352999	29	Active	Sub-urban	49.9
Cloone	53.944651	−7.7860829	60	Passive	Sub-urban	47.3
Cork	52.236575	−8.8144707	152	Passive	Rural	54.2
Donegal	54.853548	−8.0401895	156	Passive	Rural	58.7
Dublin Airport	53.433065	−6.2300683	57	Active	Urban	44.1
Emo	53.107601	−7.1983042	104	Active	Rural	47.9
Galway	53.459443	−8.7942903	45	Passive	Rural	55.3
Glanmire Road	51.901705	−8.4620361	9	Active	Urban	38.9
Henry street	52.661299	−8.6316064	9	Active	Urban	43.4
Kerry	52.358371	−9.5134263	172	Passive	Rural	50.5
Kilkenny	52.638296	−7.2676008	65	Active	Sub-urban	51.6
Kilkitt	54.072618	−6.8859336	159	Active	Rural	47.5
Louth	53.830967	−6.5284172	74	Passive	Rural	56.5
Mace Head	53.326668	−9.9044606	3	Active	Atlantic	60.4
Mohill	53.918458	−7.8824764	59	Passive	Rural	49.8
Palmerstown	53.357943	−6.3617630	20	Passive	Sub-urban	38.8
Rathmines	53.321997	−6.2671960	27	Active	Urban	45.7
Sligo	54.122192	−8.5003447	97	Passive	Rural	55.0
Tipp north	52.952582	−8.0724211	81	Passive	Rural	49.6
Tipp south	52.272570	−7.9401642	100	Passive	Rural	49.9
Valentia	51.938309	−10.240149	24	Active	Atlantic	50.2
Waterford	52.247032	−7.1416570	21	Active	Sub-urban	58.5
West Cork	51.774208	−9.3485513	181	Passive	Rural	51.3
Westmeath	53.565862	−7.1302202	83	Passive	Rural	46.8
Wexford	52.567809	−6.6084266	23	Passive	Rural	48.7
Wicklow	52.946317	−6.5350960	439	Passive	Rural	64.5

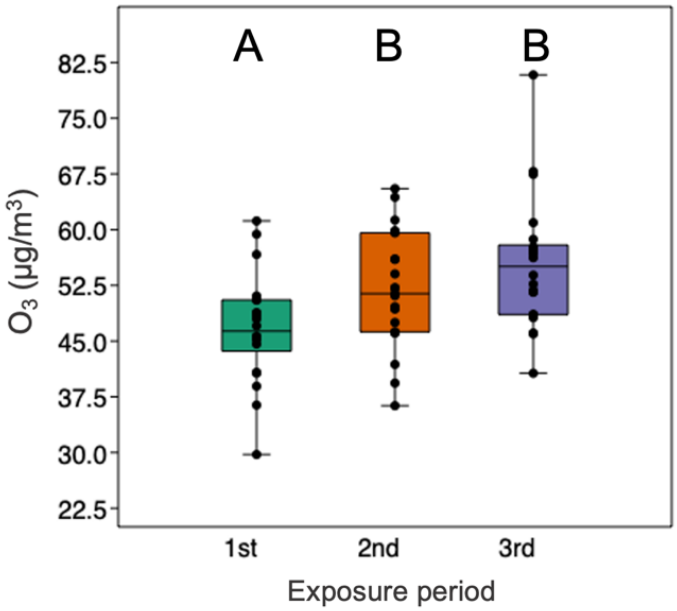

Figure 2. Monthly average ozone (O_3) concentrations for all study sites (n = 34; active = 14, passive = 20) during June, July, and August. The boxplot represents the 95th, 75th, 50th = median, 25th, and 5th percentiles. Passive samplers were deployed during four-week periods starting 13–19 June, 11–14 July, and 8–11 August, with sampling finishing on 5–8 September. Boxplot labelled "A" was significantly different (lower) from Boxplots labelled "B".

The highest summer concentration was measured at the relatively high elevation site (439 m) of Wicklow, followed by the Atlantic coastal sites of Belmullet and Mace Head (see Table 2). High elevation locations experience higher levels of O_3 as a result of the lower rate of deposition, especially overnight when temperatures are more stable [14,42]. Locations in rural areas close to coastlines experience higher O_3 levels also due to lower levels of deposition and higher insolation [43]. The lowest concentrations were measured at urban sites in Dublin and Cork city, which is consistent with previous studies in Ireland [26,28].

3.2. Predictors of O_3 in Ireland, and Insights from a Finer Spatial-Scale Concentration Map

3.2.1. Land-Use Regression Model

The final model explained 68% of the measured O_3 variance (adjusted R^2 = 0.63), and included the variables "distance to coast", "distance to Integrated Pollution Control (IPC) facility", "rain", "area of waterbodies within a radius of 1000 m", and "area of forest, woodland, and scrub within a radius 500 m" (see Table 3).

Table 3. Final land-use regression model output R^2 values and regression coefficients.

R^2	Adjusted R^2	Intercept	Dist. Coast	Dist. IPC	Rain	Forest Area 500 m	Waterbodies Area 1000 m
0.68	0.63	35.6535	−3.1137	3.5064	9.7495	−1.0596	−2.3110

The intercept is the background O_3 concentration in Ireland, around which O_3 concentration will increase or decrease in response to the effects of the predictor variables. In general, the predictor variables represented sources and sinks of O_3, and three of the five predictors had a negative slope, indicating a reducing effect on concentrations as the predictor value increased. As distance to the coast increased, O_3 concentrations decreased, which reflected the higher rate of O_3 deposition inland from the coast. Where forest, woodland, and shrubs are more common, the rate of O_3 deposition onto vegetation surfaces and within leaves is higher, leading to lower concentrations in the air. Further, forest

areas reduce ambient daytime maximum temperatures [44], which may reduce ambient O_3. Plants are a source of biogenic VOCs [45], which would be expected to increase O_3 concentrations; however, the negative slope may be explained by lower NO_x emissions in these forested areas, leading to lower O_3 production in these NOx-limited regimes [12]. As distance from IPC facilities increased, O_3 concentrations were predicted to also increase. The EPA IPC facilities are indicators of higher urban atmospheric emissions, as they are often located in urban or industrialised areas and produce a wide range of materials from metals and cement for construction to food and beverage processing [46]. These urban or industrialised areas are associated with lower O_3 concentrations from NO_x titration. While known indicators of NO_x sources such as road length and population did not increase the R^2 value sufficiently to be included in the model, IPC facilities may be associated with larger NO_x emitting centres, making them a better predictor of O_3 titration. Higher annual rainfall coincidently occurred with higher concentrations of O_3; in general, high elevation locations experience more rainfall, while O_3 is also higher in these areas due to higher rates of UV radiation and potential stratospheric intrusion [47]. The presence of waterbodies within a 1000 m buffer, including both marine and fresh waterbodies, had a negative slope. When determinants were normalised to compare their contribution individually, distance to coast had a greater effect (nearly double) than that of the area of waterbodies within 1000 m (–1.06 and –0.63 respectively), indicating that distance to coast had a greater impact on concentrations in locations where the area of waterbodies was also high.

Cross validation of the final model led to an R^2 value of 0.52; however, this value was strongly influenced by one station (Waterford) that experienced extreme O_3 concentrations during a summer heatwave. When Waterford was removed from the validation, the R^2 value increased to 0.65 (see Figure S2).

3.2.2. Modelled Ozone Concentrations

Ozone concentrations on a 1 km × 1 km spatial scale were mapped by extracting the explanatory variables at the same resolution across Ireland and combining them with the model regression coefficients to predict O_3 at centre of each grid cell. Median O_3 from the final model was 52.5 μg/m^3 (range 40.2–78.0 μg/m^3), which is higher than the measured median of 50.6 μg/m^3 (see Figure 3; Table S2; Figure S3). The lowest predicted value (40.2 μg/m^3) was also higher than the lowest measured value (38.8 μg/m^3). The areas of highest modelled values were in rural, high-elevation, and coastal areas (see Figure 4), with 3% of estimated 1 km × 1 km points (2108 km^2) above the average of the highest measured O_3 (Wicklow; 64.5 μg/m^3).

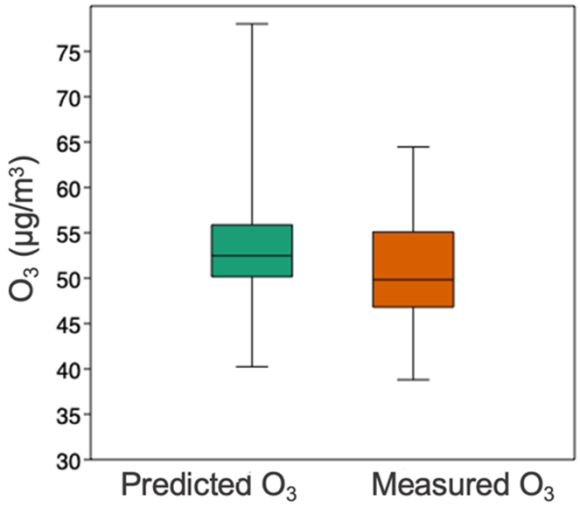

Figure 3. Summer average predicted (1 km × 1 km) and measured O_3 concentrations (active and calibrated passive) for all study sites (n = 34; active = 14, passive = 20). The boxplot represents the 95th, 75th, 50th = median, 25th, and 5th percentiles.

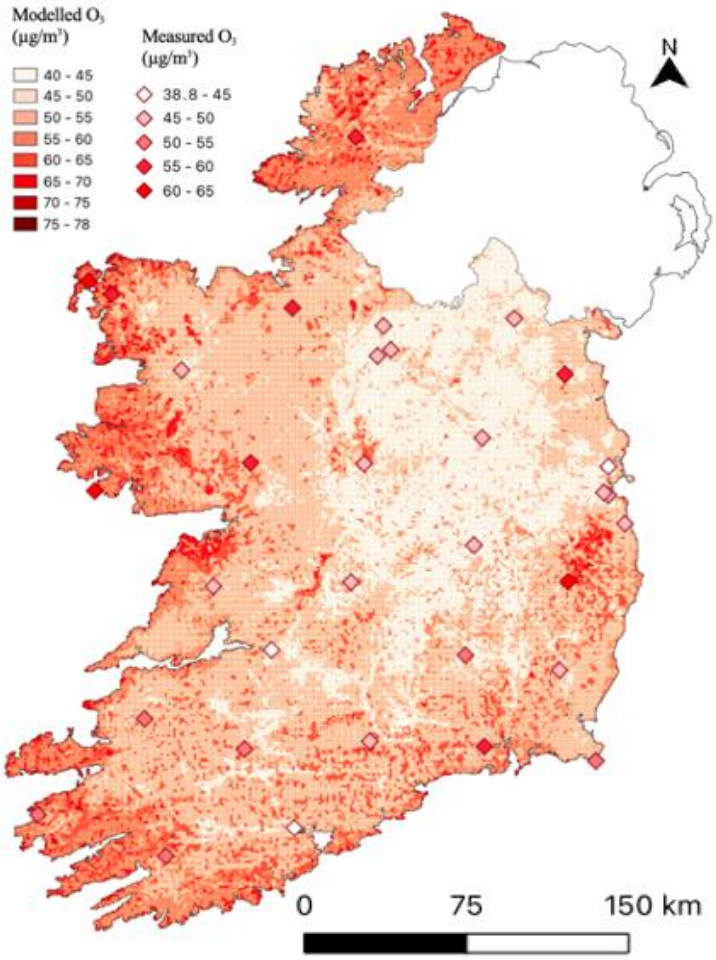

Figure 4. Modelled 1 km × 1 km and measured summer mean ozone (O_3) concentrations in the Republic of Ireland. Diamonds represent the measured concentration at each active and passive study site.

3.3. Land-Use Regression Studies

We successfully developed a land-use regression model that explained 68% of the variance in summer average O_3 concentrations (see Table 3). The efficacy of land-use regression models in predicting pollutant concentrations varies across different pollutants. Land-use regression studies for NO_2 have reported R^2 values of 0.86 [48] and 0.92 [29]. In contrast, lower values are generally reported for PM_{10} and $PM_{2.5}$ (median R^2 = 0.77 and 0.71 respectively; [31]). Particulate matter predictions are lower due to the complex mix of sources that contribute to concentrations and the formation of secondary fine PM from precursor gases. Similarly, due to the secondary-formation nature of O_3, it is more difficult to predict compared to directly emitted pollutants such as NO_2. A European study of O_3 concentrations at rural background sites achieved an R^2 value of 0.62 using a 1 km × 1 km spatial resolution [49]. A land-use regression analysis similar to this study [35], which looked at a cross section of site types, achieved a slightly better performance with an R^2 of 0.71 (adjusted R^2 0.69) and had a higher concentration for the background intercept (48.32 µg/m^3). In contrast to this study, the main drivers of concentrations in the Netherlands were related to the impact of NO_x scavenging, with traffic intensity, road length, and urban indicators included as determinants in the final model.

A recent review of O_3 modelling methods by De Marco [50], highlighted how linear regression modelling has been widely used because of the simplicity in establishing a direct relationship between the measured O_3 and local variables. However, the nonlinear nature of O_3 formation and the problem of multicollinearity in the model were highlighted as

limitations. However, as linear regression models are informed by measured observational data, they are effective compared to coarse regional chemistry–climate models, which have difficulty reproducing ground observations, and validation is limited to where ground observations are available [51].

Success of the model presented here demonstrates how land-use variables can be effectively used to predict O_3 concentrations in Ireland (see Figure 4). While the current study focused on summer average concentrations, it may be possible to increase the temporal resolution, which would be important given the variable nature of O_3 concentrations, as meteorological conditions during sampling may have caused differences between sites that may be more or less pronounced across the year. The exclusion of Northern Ireland from this study was a result of the lack of comparable predictor variables, which may be available in a future study.

4. Conclusions

Through the development of a land-use regression model, which explained 68% of the variance in summer mean O_3 concentrations, we identified covariates that represented deposition and removal processes in the Republic of Ireland. Measured concentrations varied spatially, with higher concentrations in rural upland and Atlantic areas and lower concentrations in urban centres, consistent with previous studies. The modelled 1 km × 1 km map provided a novel spatial interpretation of O_3 concentrations related to deposition environments, topography, and landcover. This study contributes to our understanding of the distribution of O_3 concentrations in Ireland, with implications for pollution control. The model demonstrates the efficacy of land-use regression in predicting secondary air pollutants, which is important for the effective protection of human and vegetation health.

Supplementary Materials: The following supporting information can be downloaded at: https://www.mdpi.com/article/10.3390/atmos14121711/s1, Table S1: Average co-located passive and active ozone data (μg/m^3) for Clonskeagh (CSK) and Kilkenny (SVL) and the reduction as % of the passive value used to calibrate the passive results; Table S2: Predictor variable values used in final model; Figure S1: The 16 existing monitoring stations (triangles) and 14 new sampling sites (circles). New sample points were chosen from the centre of spatially balanced strata that were mapped using k-means clustering in R (SPCOSA package; [36]); Figure S2: Scatter plot and R^2 values of predicted and measured ozone with Waterford site included (A) and Waterford site removed (B); Figure S3: Frequency distribution of modelled ozone data (μg/m^3) for summer 2022.

Author Contributions: Conceptualization, K.M. and J.A.; methodology, K.M., T.C. and J.A.; formal analysis, K.M.; investigation, K.M.; writing—original draft preparation, K.M.; writing—review and editing, K.M., T.C. and J.A.; project administration, T.C.; funding acquisition, T.C. All authors have read and agreed to the published version of the manuscript.

Funding: This study was funded by Environmental Protection Agency Ireland (EPA), grant number 2019-CCRP-LS.3.

Institutional Review Board Statement: Not applicable.

Informed Consent Statement: Not applicable.

Data Availability Statement: Data used in this study are available from the online database: EPA SAFER, eparesearch.epa.ie/safer/iso19115/display?isoID=66 (accessed on 15 November 2023).

Acknowledgments: The authors greatly appreciate the technical help provided by the Trent University library and archive—Maps, Data & Government Information Centre.

Conflicts of Interest: The authors declare no conflict of interest.

References

1. EEA. *Health Effects of Exposure to Ozone*; EEA Publications: Copenhagen, Denmark, 2016; Available online: https://www.eea.europa.eu/publications/TOP08-98/page010.html (accessed on 15 November 2023).

2. World Health Organization. *Review of Evidence on Health Aspects of Air Pollution: REVIHAAP Project: Technical Report (No. WHO/EURO: 2013–4101–43860-61757)*; World Health Organization, Regional Office for Europe: Geneva, Switzerland, 2021.
3. Mills, G.; Wagg, S.; Harmens, H. *Ozone Pollution: Impacts on Ecosystem Services and Viodiversity*; NERC/Centre for Ecology & Hydrology: Lancaster, UK, 2013; Available online: https://nora.nerc.ac.uk/id/eprint/502675/ (accessed on 15 November 2023).
4. Grulke, N.E.; Heath, R.L. Ozone effects on plants in natural ecosystems. *Plant Biol.* **2020**, *22*, 12–37. [CrossRef]
5. Juráň, S.; Grace, J.; Urban, O. Temporal Changes in Ozone Concentrations and Their Impact on Vegetation. *Atmosphere* **2021**, *12*, 82. [CrossRef]
6. Mills, G.; Pleijel, H.; Malley, C.S.; Sinha, B.; Cooper, O.R.; Schultz, M.G.; Neufeld, H.S.; Simpson, D.; Sharps, K.; Feng, Z.; et al. Tropospheric Ozone Assessment Report: Present-day tropospheric ozone distribution and trends relevant to vegetation. *Elem. Sci. Anthr.* **2018**, *6*, 47. [CrossRef]
7. CLRTAP. *Towards Cleaner Air. Scientific Assessment Report*; Maas, R., Grennfelt, P., Eds.; EMEP Steering Body and Working Group on Effects of the Convention on Long-Range Transboundary Air Pollution: Olso, Norway, 2016; p. 50.
8. EPA. *Ireland's Air Pollutant Emissions 1990–2030. Monotoring & Assessment: Climate Change*; Air Emissions Publications: Wexford, Ireland, 2020. Available online: https://www.epa.ie/pubs/reports/air/airemissions/irelandsairpollutantemissions2018/EPA-Air-Pollutant-Emissions-website.pdf (accessed on 15 November 2023).
9. Schumann, U.; Huntrieser, H. The global lightning-induced nitrogen oxides source. *Atmos. Chem. Phys.* **2007**, *7*, 3823–3907. [CrossRef]
10. Sillman, S. The relation between ozone, NOx and hydrocarbons in urban and polluted rural environments. *Atmos. Environ.* **1999**, *33*, 1821–1845. [CrossRef]
11. Tan, Z.; Lu, K.; Dong, H.; Hu, M.; Li, X.; Liu, Y.; Lu, S.; Shao, M.; Su, R.; Wang, H.; et al. Explicit diagnosis of the local ozone production rate and the ozone-NOx-VOC sensitivities. *Sci. Bull.* **2018**, *63*, 1067–1076. [CrossRef]
12. Wang, P.; Chen, Y.; Hu, J.; Zhang, H.; Ying, Q. Attribution of Tropospheric Ozone to NO_x and VOC Emissions: Considering Ozone Formation in the Transition Regime. *Environ. Sci. Technol.* **2018**, *53*, 1404–1412. [CrossRef]
13. Karl, T.; Lamprecht, C.; Graus, M.; Cede, A.; Tiefengraber, M.; de Arellano, J.V.-G.; Gurarie, D.; Lenschow, D. High urban NO_x triggers a substantial chemical downward flux of ozone. *Sci. Adv.* **2023**, *9*, eadd2365. [CrossRef]
14. Sicard, P.; Serra, R.; Rossello, P. Spatiotemporal trends in ground-level ozone concentrations and metrics in France over the time period 1999–2012. *Environ. Res.* **2016**, *149*, 122–144. [CrossRef]
15. Monks, P.S.; Archibald, A.T.; Colette, A.; Cooper, O.; Coyle, M.; Derwent, R.; Fowler, D.; Granier, C.; Law, K.S.; Mills, G.E.; et al. Tropospheric ozone and its precursors from the urban to the global scale from air quality to short-lived climate forcer. *Atmos. Chem. Phys.* **2015**, *15*, 8889–8973. [CrossRef]
16. Sicard, P.; De Marco, A.; Agathokleous, E.; Feng, Z.; Xu, X.; Paoletti, E.; Rodriguez, J.J.D.; Calatayud, V. Amplified ozone pollution in cities during the COVID-19 lockdown. *Sci. Total Environ.* **2020**, *735*, 139542. [CrossRef]
17. Fowler, D.; Flechard, C.; Cape, J.N.; Storeton-West, R.L.; Coyle, M. Measurements of Ozone Deposition to Vegetation Quantifying the Flux, the Stomatal and Non-Stomatal Components. *Water Air Soil Pollut.* **2001**, *130*, 63–74. [CrossRef]
18. Garland, J.A.; Derwent, R.G. Destruction at the ground and the diurnal cycle of concentration of ozone and other gases. *Q. J. R. Meteorol. Soc.* **1979**, *105*, 169–183. [CrossRef]
19. Fowler, D.; Pilegaard, K.; Sutton, M.; Ambus, P.; Raivonen, M.; Duyzer, J.; Simpson, D.; Fagerli, H.; Fuzzi, S.; Schjoerring, J.; et al. Atmospheric composition change: Ecosystems–Atmosphere interactions. *Atmos. Environ.* **2009**, *43*, 5193–5267. [CrossRef]
20. Blanchard, D.; Aherne, J. Spatiotemporal variation in summer ground-level ozone in the Sandbanks Provincial Park, Ontario. *Atmos. Pollut. Res.* **2019**, *10*, 931–940. [CrossRef]
21. Agyei, T.; Juráň, S.; Ofori-Amanfo, K.K.; Šigut, L.; Urban, O.; Marek, M.V. The impact of drought on total ozone flux in a mountain Norway spruce forest. *J. For. Sci.* **2020**, *66*, 280–278. [CrossRef]
22. Schultz, M.G.; Schröder, S.; Lyapina, O.; Cooper, O.R.; Galbally, I.; Petropavlovskikh, I.; von Schneidemesser, E.; Tanimoto, H.; Elshorbany, Y.; Naja, M.; et al. Tropospheric Ozone Assessment Report: Database and metrics data of global surface ozone observations. *Elem. Sci. Anthr.* **2017**, *5*, 58. [CrossRef]
23. Young, P.J.; Archibald, A.T.; Bowman, K.W.; Lamarque, J.-F.; Naik, V.; Stevenson, D.S.; Tilmes, S.; Voulgarakis, A.; Wild, O.; Bergmann, D.; et al. Pre-industrial to end 21st century projections of tropospheric ozone from the Atmospheric Chemistry and Climate Model Intercomparison Project (ACCMIP). *Atmos. Meas. Tech.* **2013**, *13*, 2063–2090. [CrossRef]
24. Derwent, R.G.; Utembe, S.R.; Jenkin, M.E.; Shallcross, D.E. Tropospheric ozone production regions and the intercontinental origins of surface ozone over Europe. *Atmos. Environ.* **2015**, *112*, 216–224. [CrossRef]
25. Proietti, C.; Fornasier, M.F.; Sicard, P.; Anav, A.; Paoletti, E.; De Marco, A. Trends in tropospheric ozone concentrations and forest impact metrics in Europe over the time period 2000–2014. *J. For. Res.* **2021**, *32*, 543–551. [CrossRef]
26. McHugh, K.; Cummins, T.; Aherne, J. Distribution and Long-Term Trends of Tropospheric Ozone Concentrations in Ireland. *Atmosphere* **2023**, *14*, 569. [CrossRef]
27. Derwent, R.G.; Manning, A.J.; Simmonds, P.G.; Spain, T.G.; O'Doherty, S. Analysis and interpretation of 25 years of ozone observations at the Mace Head Atmospheric Research Station on the Atlantic Ocean coast of Ireland from 1987 to 2012. *Atmos. Environ.* **2013**, *80*, 361–368. [CrossRef]

28. Tripathi, O.P.; Jennings, S.G.; O'dowd, C.; O'leary, B.; Lambkin, K.; Moran, E.; O'Doherty, S.J.; Spain, T.G. An assessment of the surface ozone trend in Ireland relevant to air pollution and environmental protection. *Atmos. Pollut. Res.* **2012**, *3*, 341–351. [CrossRef]
29. Beelen, R.; Hoek, G.; Vienneau, D.; Eeftens, M.; Dimakopoulou, K.; Pedeli, X.; Tsai, M.-Y.; Künzli, N.; Schikowski, T.; Marcon, A.; et al. Development of NO^2 and NOx land use regression models for estimating air pollution exposure in 36 study areas in Europe—The ESCAPE project. *Atmos. Environ.* **2013**, *72*, 10–23. [CrossRef]
30. de Hoogh, K.; Wang, M.; Adam, M.; Badaloni, C.; Beelen, R.; Birk, M.; Cesaroni, G.; Cirach, M.; Declercq, C.; Dėdelė, A.; et al. Development of Land Use Regression Models for Particle Composition in Twenty Study Areas in Europe. *Environ. Sci. Technol.* **2013**, *47*, 5778–5786. [CrossRef]
31. Eeftens, M.; Tsai, M.-Y.; Ampe, C.; Anwander, B.; Beelen, R.; Bellander, T.; Cesaroni, G.; Cirach, M.; Cyrys, J.; De Hoogh, K.; et al. Spatial variation of PM2.5, PM10, PM2.5 absorbance and PMcoarse concentrations between and within 20 European study areas and the relationship with NO2—Results of the ESCAPE project. *Atmos. Environ.* **2012**, *62*, 303–317. [CrossRef]
32. Gilbert, N.L.; Goldberg, M.S.; Beckerman, B.; Brook, J.R.; Jerrett, M. Assessing Spatial Variability of Ambient Nitrogen Dioxide in Montréal, Canada, with a Land-Use Regression Model. *J. Air Waste Manag. Assoc.* **2005**, *55*, 1059–1063. [CrossRef]
33. Jones, R.R.; Hoek, G.; Fisher, J.A.; Hasheminassab, S.; Wang, D.; Ward, M.H.; Sioutas, C.; Vermeulen, R.; Silverman, D.T. Land use regression models for ultrafine particles, fine particles, and black carbon in Southern California. *Sci. Total Environ.* **2020**, *699*, 134234. [CrossRef]
34. Mo, Y.; Booker, D.; Zhao, S.; Tang, J.; Jiang, H.; Shen, J.; Chen, D.; Li, J.; Jones, K.C.; Zhang, G. The application of land use regression model to investigate spatiotemporal variations of PM2.5 in Guangzhou, China: Implications for the public health benefits of PM2.5 reduction. *Sci. Total Environ.* **2021**, *778*, 146305. [CrossRef]
35. Kerckhoffs, J.; Wang, M.; Meliefste, K.; Malmqvist, E.; Fischer, P.; Janssen, N.A.; Beelen, R.; Hoek, G. A national fine spatial scale land-use regression model for ozone. *Environ. Res.* **2015**, *140*, 440–448. [CrossRef]
36. Walvoort, D.; Brus, D.; de Gruijter, J. Spcosa: Spatial Coverage Sampling and Random Sampling from Compact Geographical Strata. R package Version 0.4–2. 2023. Available online: https://CRAN.R-project.org/package=spcosa (accessed on 15 November 2023).
37. Lefohn, A.S.; Malley, C.S.; Smith, L.; Wells, B.; Hazucha, M.; Simon, H.; Naik, V.; Mills, G.; Schultz, M.G.; Paoletti, E.; et al. Tropospheric ozone assessment report: Global ozone metrics for climate change, human health, and crop/ecosystem research. *Elem. Sci. Anthr.* **2018**, *6*, 27. [CrossRef]
38. Scheeren, B.A.; Adema, E.H. Monitoring ambient ozone with a passive measurement technique method, field results and strategy. *Water Air Soil Pollut.* **1996**, *91*, 335–350. [CrossRef]
39. MapEire. MapEIre—"National Mapping of GHG and Non–GHG Emissions Sources Project". Available online: https://projects.au.dk/mapeire/spatial-results/ (accessed on 15 November 2023).
40. Yoshioka, K. KyPlot—A User-oriented Tool for Statistical Data Analysis and Visualization. *Comput. Stat.* **2002**, *17*, 425–437. [CrossRef]
41. Wang, M.; Beelen, R.; Eeftens, M.; Meliefste, K.; Hoek, G.; Brunekreef, B. Systematic Evaluation of Land Use Regression Models for NO_2. *Environ. Sci. Technol.* **2012**, *46*, 4481–4489. [CrossRef]
42. Agathokleous, S.; Saitanis, C.J.; Savvides, C.; Sicard, P.; Agathokleous, E.; de Marco, A. Spatiotemporal variations of ozone exposure and its risks to vegetation and human health in Cyprus: An analysis across a gradient of altitudes. *J. For. Res.* **2023**, *34*, 579–594. [CrossRef]
43. Pleijel, H.; Klingberg, J.; Karlsson, G.P.; Engardt, M.; Karlsson, P.E. Surface Ozone in the Marine Environment—Horizontal Ozone Concentration Gradients in Coastal Areas. *Water Air Soil Pollut.* **2013**, *224*, 1603. [CrossRef]
44. Baldocchi, D.; Ma, S. How will land use affect air temperature in the surface boundary layer? Lessons learned from a comparative study on the energy balance of an oak savanna and annual grassland in California, USA. *Tellus B Chem. Phys. Meteorol.* **2013**, *65*, 19994. [CrossRef]
45. Fall, R. Biogenic Emissions of Volatile Organic Compounds from Higher Plants. In *Reactive Hydrocarbons in the Atmosphere*; Academic Press: Cambridge, MA, USA, 1999; pp. 41–96. [CrossRef]
46. EPA. Licencing & Permitting: "Integrated Pollution Control (IPC) Publications". 2020. Available online: https://www.epa.ie/publications/licensing{-}{-}permitting/industrial/ipc/first-schedule-to-the-epa-act-1992-as-amended.php (accessed on 15 November 2023).
47. Lefohn, A.S.; Wernli, H.; Shadwick, D.; Oltmans, S.J.; Shapiro, M. Quantifying the importance of stratospheric-tropospheric transport on surface ozone concentrations at high- and low-elevation monitoring sites in the United States. *Atmos. Environ.* **2012**, *62*, 646–656. [CrossRef]
48. Eeftens, M.; Beelen, R.; Fischer, P.; Brunekreef, B.; Meliefste, K.; Hoek, G. Stability of measured and modelled spatial contrasts in NO^2 over time. *Occup. Environ. Med.* **2011**, *68*, 765–770. [CrossRef]
49. Beelen, R.; Hoek, G.; Pebesma, E.; Vienneau, D.; de Hoogh, K.; Briggs, D.J. Mapping of background air pollution at a fine spatial scale across the European Union. *Sci. Total Environ.* **2009**, *407*, 1852–1867. [CrossRef]

50. De Marco, A.; Garcia-Gomez, H.; Collalti, A.; Khaniabadi, Y.O.; Feng, Z.; Proietti, C.; Sicard, P.; Vitale, M.; Anav, A.; Paoletti, E. Ozone modelling and mapping for risk assessment: An overview of different approaches for human and ecosystems health. *Environ. Res.* **2022**, *211*, 113048. [CrossRef]
51. Sicard, P.; Crippa, P.; De Marco, A.; Castruccio, S.; Giani, P.; Cuesta, J.; Paoletti, E.; Feng, Z.; Anav, A. High spatial resolution WRF-Chem model over Asia: Physics and chemistry evaluation. *Atmos. Environ.* **2021**, *244*, 118004. [CrossRef]